

The Exeter Partnerships:
An Insider's Comments on Effectiveness

Submitted by Mukondraj Khetani to the University of Exeter
as a dissertation for the degree of
Master of Philosophy in Physics
In September 2017

This dissertation is available for Library use on the understanding that it is
copyright material and that no quotation from the thesis may be published
without proper acknowledgement.

I certify that all material in this thesis which is not my own work has been
identified and that no material has previously been submitted and approved for
the award of a degree by this or any other University.

Signature:

*Implementing graphene and other materials into Cash in transit (CIT) boxes to
enhance security*

Contents

Abstract.....	4
Introduction and background.....	5
What is Graphene?	5
Mechanical properties	6
Chemical properties.....	7
Electrical properties	7
Optical properties.....	7
Graphene inks	7
Graphene Dispersed in Liquid.....	7
Conductive films	7
Graphene oxide films.....	7
Electroplated films	9
Other conductive inks	10
Metal based Inks.....	10
Screen printing.....	11
PEDOT:PSS	12
LDS technology	12
Experimental and results.....	13
Methodology, materials, and equipment.....	13
Silver ink screen printing trial	16
Thermo-foldable ink trial	17
PEDOT:PSS material testing and comparison with Graphene	20
PEDOT:PSS Industrial large scale printing	21
Inkjet/Spray Printing.....	24
Electronics	26
Time-domain Reflectometry (TDR)	26
Patterns.....	31
Ladder Network.....	33
Conclusion	34
References.....	35
Bibliography	37

Table of figures

Figure 1 Graphite crystalline electronic structure (three planar sp ² orbitals and one p orbital) of one of the atoms marked (Mitura, 2006).....	5
Figure 2 A General indicator for the number of layers in a Graphene sample using Raman spectroscopy (Davim, 2012)	6
Figure 3 Graphite to Graphene via exfoliation and oxidisation (GHAFFARZADEH, 2012).....	8
Figure 4 rGO by a laser	9
Figure 5 electrolytic plating a flexible substrate with copper (Dietz, 2012).....	9
Figure 6 Electro less copper deposition solution & Electrolytic vs electro-less plating (The university of wisconsin, 2010) (NiTEC, 2015)	10
Figure 7 Thermo-foldable conductive ink.....	10
Figure 8 Systematic guide of screen printing	11
Figure 9 LDS process.....	12
Figure 10 Exfoliated graphene in water A) With surfactant B) Without surfactant (Pu, et al., 2012)	13
Figure 11 How Surfactants isolate graphene flakes.....	13
Figure 12 Graphene dispersions.....	14
Figure 13 Raman spectroscopy of LPE with surfactants	15
Figure 14 High speed shear LPE	16
Figure 15 Vacuum form ABS with screen printed silver ink	18
Figure 16 1 inch sample serpentine patterns created by photo-lithography	19
Figure 17 (Reactive Ion Etching (RIE) - Oxford Instruments)	20
Figure 18 Electrical conductivity comparison	21
Figure 19 Graphene Bend Test (Bointon et al., 2015)	21
Figure 20 Mayer bar stainless steel rod.....	22
Figure 21 Mayer bar coating	22
Figure 22 (Heraeus, 2013)	23
Figure 23 GO-Polymer Nanocomposite.....	25
Figure 24 A simple TDR workbench setup	27
Figure 25 Various TDR reflection waves, V = Voltage. (Emworks, 2017)	28
Figure 26 Trigger circuitary	29
Figure 27 All the signals from a TDR system on the right.....	29
Figure 28 Internal circuitary of the microcontroller	30
Figure 29 (David D. Eaton, David R. Staab, Ruben C. Zeta, 2011)	32
Figure 30 Capacitive spiral pattern, each colour is an isolated terminal	32
Figure 31 Ladder pattern, designed on AutoCAD	33

Abstract

Graphene was said to adhere to substrates due to strong pi-pi forces; therefore the ability to stick to polypropylene was tested. (Koenig et al., 2011) [6]. The ability of Graphene to adhere to most materials is true. However, these forces are only ultra-strong for mechanically exfoliated pristine Graphene. When Graphene is contaminated by molecules, the adhesion with the substrate is diminished. As the process of liquid exfoliated of Graphene consists of many areas of contamination, the Graphene electrodes are another part of this study. Many methods of producing Graphene electrodes are being investigated: film growth and etch, large scale conductive Graphene inks and reduction of graphene oxide. The study moved towards Silver inks as it provide far better materials specifications, for the application as a security tamper sensor for Spinnaker International. This study also goes into great depth of the electronics, which were designed to provide better sensing abilities using less power. A power consumption naturally goes up with any material other than solid copper.

Introduction and background

Cash in transit (CIT) boxes have become increasingly prone to sophisticated attacks. Thieves are reverting to methods other than brute force, to access bank notes or any legal tender. This pushes CIT box design engineers to create further elaborated sensing and cash degrading abilities. Graphene is said to be flexible, stretchable, strong, electrically conductive, and transparent. These features of various Graphene types will be examined, to assess whether they have a feasible role in CIT security. The main application requirement was for an electrode, a flexible large PCB lining. This lining can electronically identify an occurrence of physical tamper to the CIT boxes, by using newly developed electronics, specially for this study. Change in materials for the PCB lining (Copper to Graphene or other), upgrade in electronics for the tamper sensing are both key elements of this study. As this project was over-shadowed by an industry, there were many factors that controlled the decisions that were taken; such as, cost, availability of supply and ease of use, to name a few. As a result, Graphene was analysed against PEDOT:PSS and Silver inks.

What is Graphene?

Graphene is made of pure carbon in which the carbon atoms are arranged in a honeycomb pattern within a single layer. Several sheets of graphene form a stack of the well-known Graphite, held together with Van der Waals forces or p orbitals. Each layer is a honeycomb structure of carbons which are formed up of sp^2 orbitals, seen in Figure 1.

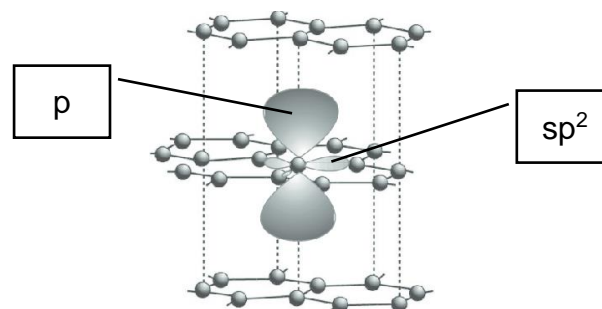


Figure 1 Graphite crystalline electronic structure (three planar sp^2 orbitals and one p orbital) of one of the atoms marked (Mitura, 2006)

Graphene consists of several useful properties such as, high: electron mobility, thermal conductivity, tensile strength and more. It conducts heat and electricity as well as being the strongest and flexible material known to man, yet it is

transparent. Figure 2 shows the data from one of the common methods used to identify graphene quality and the stacked number of layers in a sample.

Raman spectroscopy is a method used to analyse molecular vibrations in a system. This works by shining a laser beam (visible, near infrared or near ultraviolet) onto a material, whilst collecting electromagnetic radiation from the beam spot through a monochromator. Photons become 'excited' in the material, and these can be monitored. The prominent identifiers of carbons in the Raman spectra are called the G and D peaks. These are found at 1560 cm^{-1} and 1360 cm^{-1} , respectively.

The D peak is considered the defective marker, the 2D peak marks the breathing of hexagonal structure of carbons and the G peak shows a more graphitic structure. The ratio between 2D/G can give an estimate of the number of layers seen. The width and shape of the 2D peak can also be used to further estimate the number of layers.

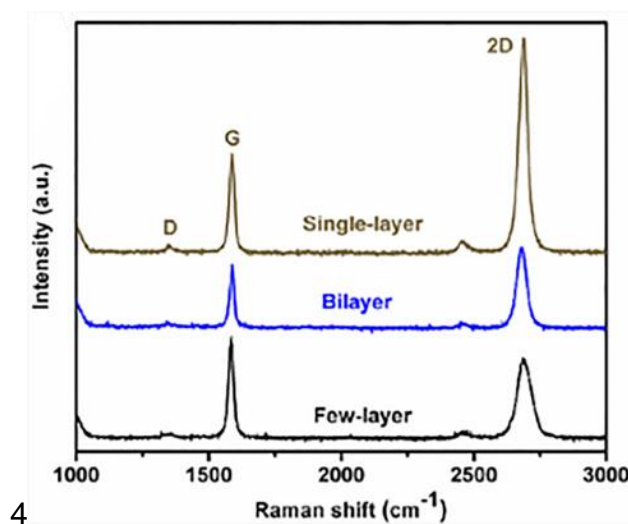


Figure 2 A General indicator for the number of layers in a Graphene sample using Raman spectroscopy (Davim, 2012)

Mechanical properties

Tensile strength: 130 GPa

Young's modulus: 0.5 - TPa

Tension rigidity: 340 GPa·nm

Surface tension: 54.8 mN/m⁸

Flexural rigidity: 3.18 GPa·nm³

Thermal conductivity: 2-4 kW·m⁻¹K⁻¹ (freely suspended graphene)

Distance between adjacent layers of graphene in graphite: 3.4 Å

Chemical properties

Burn temperature: 350 °C (662 °F)

Specific surface area: 1168 m²·g⁻¹

Electrical properties

Band gap: 0 eV (in sheet graphene)

Band gap: ~3.8 eV (in graphene ribbons)

Electron mobility: ~200,000 cm²·V⁻¹·s⁻¹ (intrinsic limit)

Electron mobility: ~40,000 cm²·V⁻¹·s⁻¹ (on SiO₂ substrate)

Carrier density: 10¹² cm⁻²

Free path for electron-acoustic phonon scattering: >2 μm

Optical properties

White light absorption: 2.3 %

White light transmission: 97.7 %

(Graphenea, 2017)

Graphene inks

Graphene Dispersed in Liquid

Graphene flakes dispersed in a liquid, usually de-ionised (di) water or a solvent, is fabricated by a method called liquid exfoliation. This is achieved by mixing bulk graphite into a liquid and using an external force to break the previously mentioned Van der Waals forces. The equipment used is an ultrasonic bath, which is commonly found in clean room labs. This method generates many flakes, relatively quickly and of a pristine quality. However, flake diameter is lost due to the nature of the process; however, for some applications this is not an issue.

Liquid exfoliation can be scaled up to produce gallons of dispersed graphene, which is why industry favours this method. The main property that can be utilised in liquid dispersed graphene is mechanical strength. When it is combined with either polymers or cement, it can drastically increase the material's tensile strength. Research in this field is still very new however, it shows promising results for the structural materials industry.

Conductive films

Graphene oxide films

Graphite can be chemically oxidised to produce graphite oxide. Oxidisation attaches functional oxygen groups to the graphite layers, which allows graphite oxide to be dispersed in water. Liquid exfoliation without solvents or surfactants,

simply in water, breaks down graphite oxide to graphene oxide (GO). (Hummers & Offeman, 1958) Figure 3 shows a visual diagram of how one can fabricate between graphene, graphite, graphene oxide and graphite oxide.

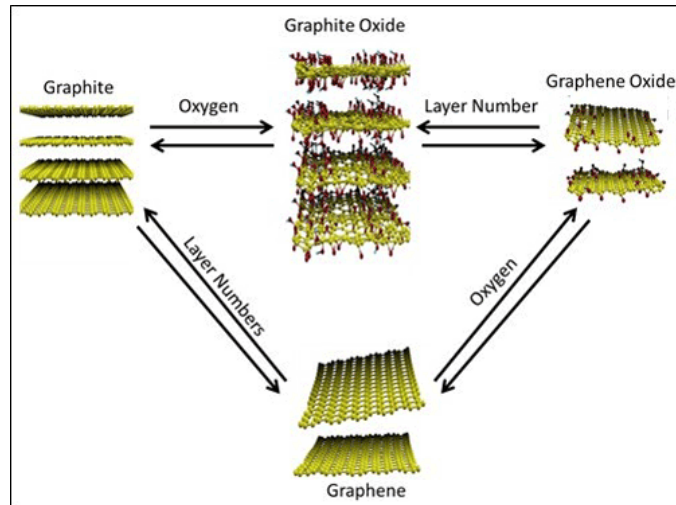


Figure 3 Graphite to Graphene via exfoliation and oxidisation
(GHAFFARZADEH, 2012)

Once there is a significant percentage of GO layers in the solution, the liquid is pumped through a filter to collect the layers into a film. The equipment used is called a vacuum filtration device, used with a 0.2um pore size filter paper. The film and filter paper stack is left to dry, which can take only 20 minutes, and a visible colour change from black to brown may be seen. The next step is to submerge the dry film and filter paper into di water, which separates the two. Thereafter, the GO film can be scooped out on to a substrate of choice. Lastly, to transform GO to Graphene, the oxygen groups must be removed, which can be achieved using various methods. For this project, patterning was needed and thus reduced GO (rGO) was created using a computer-aided laser. GO is a natural insulator which allows isolation for the electrons to travel along the rGO canal, just as it would on a flexible printed circuit board (PCB). Figure 4 shows a square section on GO that was reduced by a laser, as a proof of concept. The electrical resistance was measured using a probe station, $R = \sim 1\text{k}\Omega/\square$.

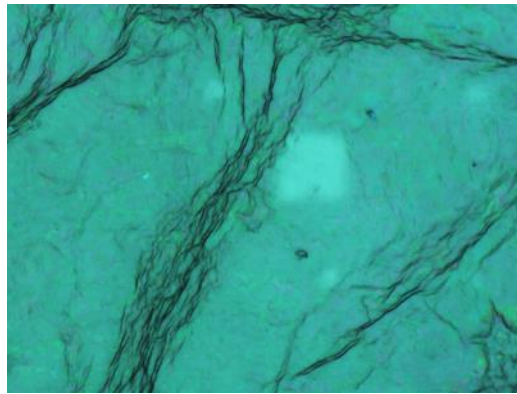


Figure 4 rGO by a laser

Electroplated films

Modern electrolytic plating has been utilised since 1805. It is a common method used to deposit copper and nickel onto desired substrates. Figure 5 shows a diagram of how copper is deposited onto a flexible substrate, such as polypropylene or polycarbonate.

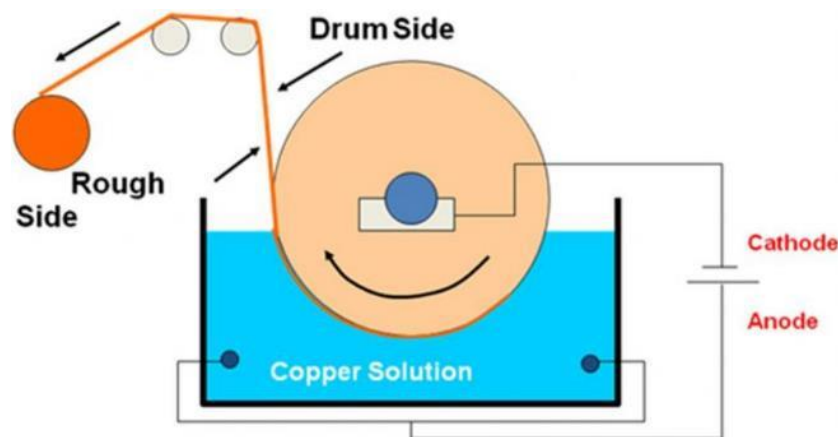


Figure 5 electrolytic plating a flexible substrate with copper (Dietz, 2012)

Another widely used method is electroless deposition, which plates substrate using a chemical-only process. This method is widely used to metallise materials in order to protect it from corrosion and to make it conduct electricity. Nickel can readily plate even non-metallic substrates however; copper plating requires a catalyst such as palladium. This must be pre-coated on the surface for an even plating. (Senese, 2010) The right-hand diagram on Figure 6 shows the uniformity that electro-less plating has in comparison to electrolytic.

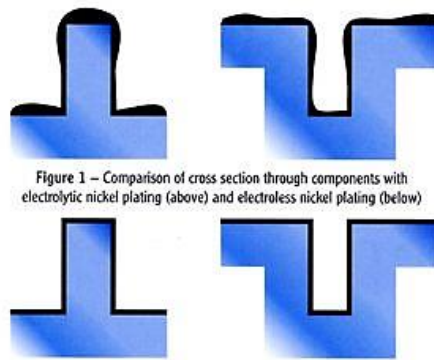
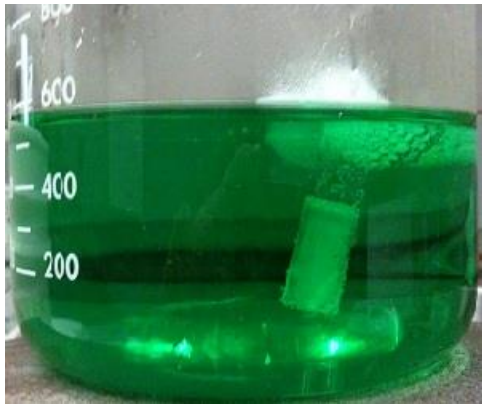


Figure 1 – Comparison of cross section through components with electrolytic nickel plating (above) and electroless nickel plating (below)

Figure 6 Electro less copper deposition solution & Electrolytic vs electro-less plating (The university of wisconsin, 2010) (NiTEC, 2015)

Other conductive inks

Screen, inkjet, and spray coating are some of the techniques used to apply conductive inks to a substrate. Viscosity of the ink greatly determines the coating method used. However, some inks can be diluted using solvents to enable other coating processes such as: flexographic, gravure and roll-to-roll screen printing. Nowadays, manufacturers like DuPont, Sun Chemicals and Henkel have commercialised a wide selection of inks designed to fit the customers' needs with minimal limitations.

Metal based Inks

Conductive metal-based inks contain three main ingredients: a functional conductive metal, some resin to allow adhesion to substrates, and a solvent to control the viscosity. As conductive inks will always have a polycrystalline metallic structure, properties such as conductivity can never be compared to crystalline metals. The resin and solvent are electrically insulating, but are required to hold the ink in place. However, conductive inks have many benefits, including flexibility, low weight, transparency, and thermo-mould ability (Figure 7).

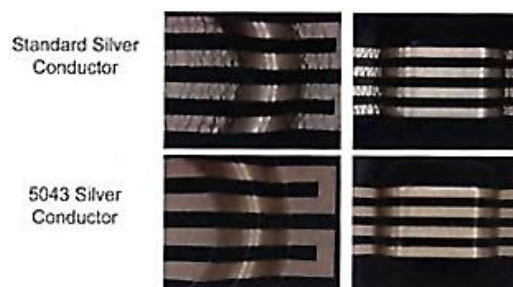


Figure 7 Thermo-foldable conductive ink

DuPont, SunChemical and Henkel were the three Silver ink suppliers that were compared in terms of cost, ink properties, and availability. The house of quality

(HOQ) rank was used to help maintain the correct priorities when choosing the product. For this project, Henkel’s Loctite 1010 was chosen as it cost the least per gram, combined with the lowest electrical resistivity at 0.007 ohms / □. (Henkel, 2016)

Screen printing

Screen printing originated from China 960–1279 AD, where some believe that the mesh was formed using human hair. Nowadays, stainless steel or polyester are the most common materials used for the mesh. The mesh essentially acts as a stencil for the ink to pass through. With a fully open mesh, the ink would pass through, printing a useless filled block image. However, a pattern can be made by applying a uniform layer of photo emulsion on top of the mesh. This emulsion layer is then put through a curing process. This hardens the layer, which is occurs by exposure to UV radiation. Sections of the emulsion (the image) is protected from UV exposure by being covered by a design mask of the required image printed on clear acetate. Once protected, the full screen is exposed to UV radiation, where the unprotected areas (negative image) harden. The soft areas are then removed by passing the screen through water jets. This consequently produces a prepared screen mesh with your desired pattern, which can be used multiples times to print the desired image. When screen printing is carried out for image at high resolution, there are several critical factors which can affect the result: mesh count, thickness of the photo emulsion layer, pressure, and the angle of the squeegee. (Gwent Group, 2017). [OBJ]Figure 88[OBJ] shows the . (James C. Y. Watt, Anne E. Wardwell, Morris Rossabi, 1999)

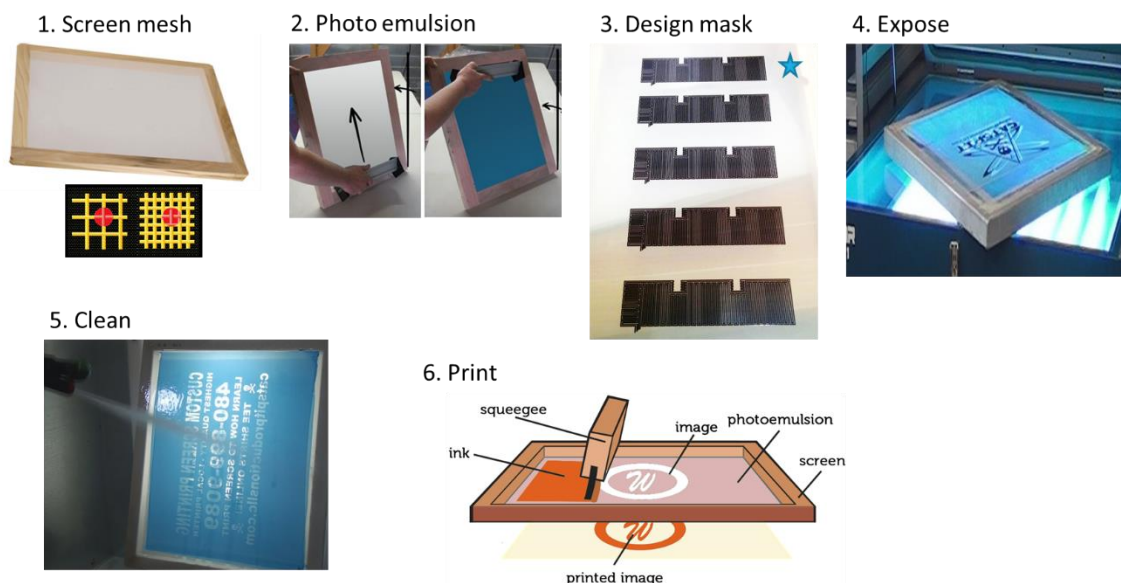


Figure 8 Systematic guide of screen printing

PEDOT:PSS

The two primary reasons for the project diverting to the use of PEDOT:PSS is due to its scalability and relatively low electrical resistance of $25\Omega/\square$ when coated on Polyethylene terephthalate (PET) sheets. In comparison, CVD graphene measures at $1k\ \Omega/\square$ on PET at best (Neves et al., 2015).

PEDOT:PSS is a conductive polymer, poly(3,4-ethylene dioxy-thiophene) (PEDOT) doped with poly(styrene sulfonate) (PSS) – both have transparent properties that varies with thickness. (Alemu et al., 2012) PEDOT:PSS's conductivity can be deactivated by applying a low 1% dose of Sodium Hypochlorite for 5 seconds. A quick water wash is required, straight after for the passivation to stop; otherwise full etching starts to occur. This destruction of conductivity is called passivation, because only the conductivity is lost yet the materials stays intact on the base surface. Some slight discoloration does occur, yet it is so faint to the naked eye. Optimising the concentration and etching time, can provide superior results, required for the application. By using a widely used photolithography technique, conductive patterns can be designed into the PEDOT:PSS whilst hidden to the eye. (AGFA, 2001)

LDS technology

LDS (Laser Direct Structuring) is a special process that utilises the ability of structuring doped thermoplastic by using a laser, to create a conductive path prior to copper electroplating. This allows circuits to be laid out three-dimensional structures. There are huge benefits to this as electronic circuitry can be placed in tight confinements, opening up space for devices. Figure 9 shows the LDS steps for further understanding.

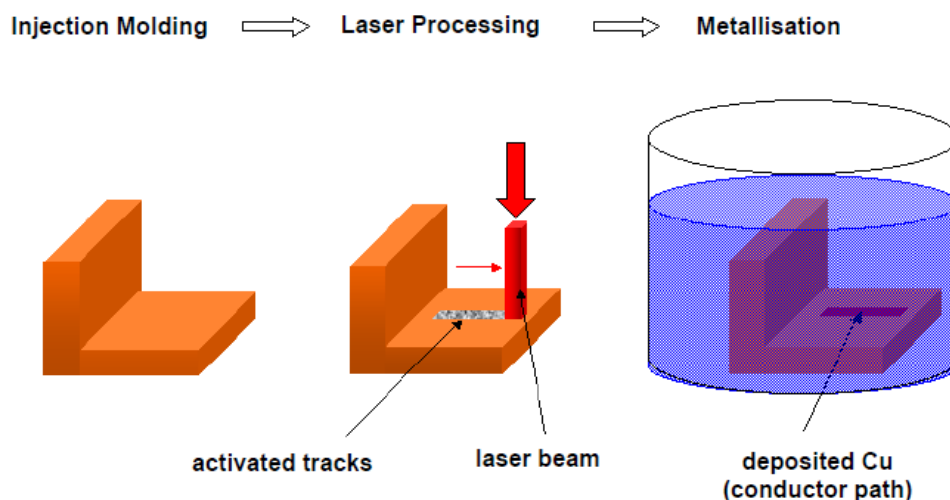


Figure 9 LDS process

Experimental and results

Methodology, materials, and equipment

Graphite powder can be purchased from Sigma Aldrich in various particle sizes. For this study particle size of <20nm was used to attain the thinnest graphene flakes possible. Graphite is then mixed with di-water, but as water's surface energy is too high to exfoliate graphene, surfactants are added to lower the surface energy, which not only aids exfoliation, but also disperses graphene flakes to create a colloidal system. The difference is shown below in Figure 10.

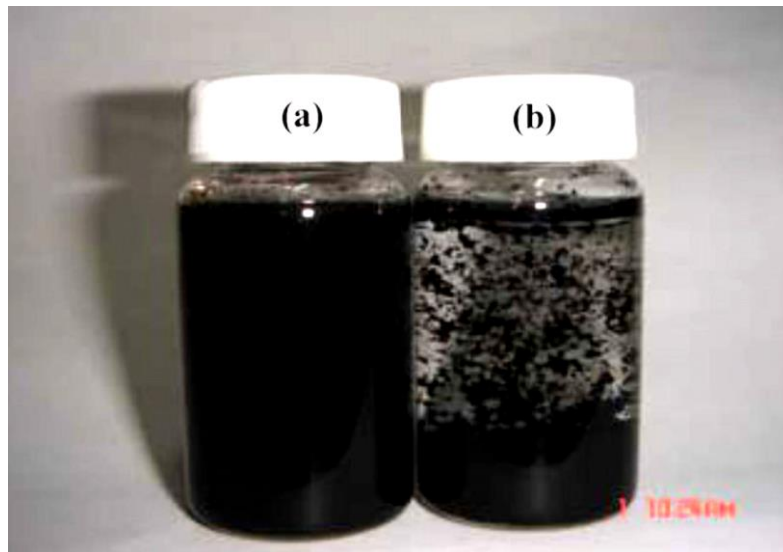


Figure 10 Exfoliated graphene in water A) With surfactant B) Without surfactant (Pu, et al., 2012)

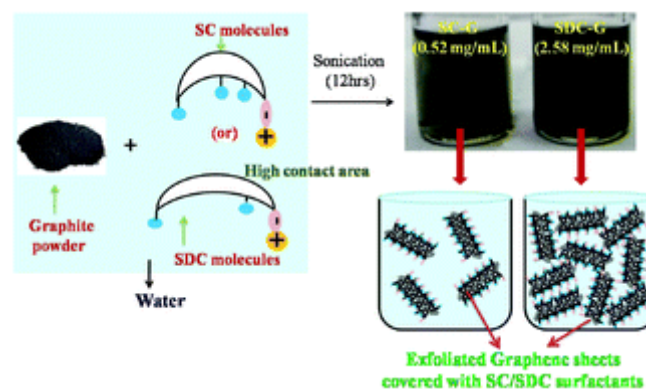


Figure 11 How Surfactants isolate graphene flakes

Figure 11 shows how the two main surfactants, sodium cholate (SC) or sodium deoxycholate (SDC), are used with graphite to isolate graphene. (Ramalingam et al., 2013)

Solvents

Other than water, solvents such as NMP, Gamma Butyrolactone and IPA can be used to liquid exfoliate graphite. These do not require surfactants, as the surface energy of the solvents is low enough to promote exfoliation. Surfactants change some of the properties of the exfoliated graphene, such as lowering the electrical conductivity, which makes solvents a suitable alternative. The required application of a long serpentine electrode will have a large total resistance; therefore, it is highly important to minimise the electrical resistance at its material level.

Ultrasonic Exfoliation

The surfactants, combined with water or a solvent, are mixed in a beaker with various ratios and then placed in an ultrasonic bath. The sonication weakens the sp^3 bonds and separates the graphene sheets. Various ratios produce various qualities of graphene flakes; therefore, it is key to optimise these ratios for each set up. Figure 12 shows two small solutions that were produced, each with a slightly different method – for the solution on the left-hand-side, the surfactant SD was added to the graphite water solution in increments, whereas the solution on the right-hand-side had 0.05g of SD added at the very beginning. Both samples were sonicated next to each other 8 hours, to minimise any other factors. The samples are placed in front of a paper with the collaborators logos on Figure 12, to prove transparency of the solutions. When looked at closely, thin graphite flakes can be seen, as the solution contains a mixture of thin graphite, few layer graphene (FLG), bi-layer graphene and single layer graphene (SLG).



Figure 12 Graphene dispersions

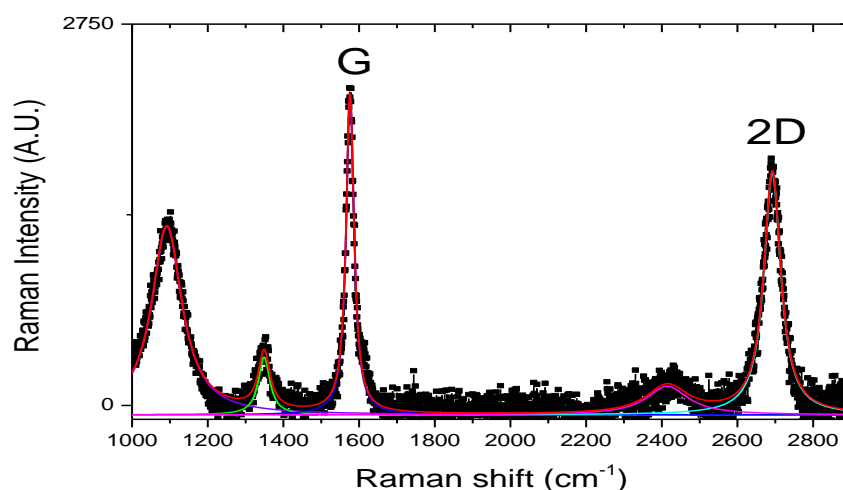


Figure 13 Raman spectroscopy of LPE with surfactants

Figure 13 shows the analysed data generated by a Raman spectrometer of a flake from the SC incremented sample. The ratio between 2D and G peak provides a basic idea of the number of layers. As the G peak is larger than the 2D peak, this flake would not be SLG. As the ratio is 2D/G 0.86, this is more likely to be FLG; which can be used for producing the electrode. If you compare these results to (Pu, et al., 2012) who carried out Raman analysis on thermal reduced graphene, you can see that these is a must high d-peak ratio on their study. This would be because the thermal reduction process would be damaging or removing carbon atoms. Therefore, LPE is a much better fabrication process that keeps Graphene quality at its best. High quality results in high conductivity, flexibility and strength.

It was evident that the sample where the addition of SC was incremented over a period of time, produced a larger number of colloidal flakes. There is not any literature of this however, the assumption would be that the SC is damaged by the sonication, and by adding fresh SC helps with the isolation of flakes. Whereas, the no incremented samples had far more graphite left, which was filtered out though the standard vacuum filtration step.

High Speed Shear Exfoliation

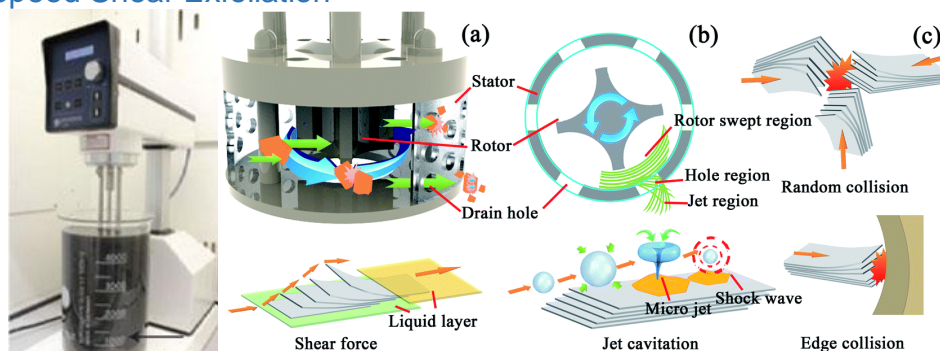


Figure 14 High speed shear LPE

High speed shear exfoliation is another method that has been used more recently to produce larger quantities of colloidal solutions in a shorter period. This device Silverion model L5M works like a kitchen blender, where random collision, shear force, jet cavitation and edge collision all take part in breaking the graphite layers apart. Figure 14 High speed shear LPE above, shows the forces that the graphite flakes experience during shear exfoliation. This method is said to produce flakes with much lower defects and larger flakes in diameter, which is analysed by looking at the defective peak or the D peak. Having a lower defective peak suggests two things. Firstly, it could be a sign of a large flake as a flake edge nearby the Raman laser beam spot, recognises as a defect; due to the missing carbon atoms. Secondly, a carbon atom missing in the centre. However, it is very uncommon that any type graphene exfoliation has missing carbon atoms around the centre; therefore d-peak defects also gives a good indication of flake size. Large flakes have better conductivity over a larger span, when using in an ink or paste. (Paton, 2014) where the first to use utilise high speed shear exfoliation, and their results were identical to the ones in this study, which shows the experiment is repeatable.

Silver ink screen printing trial

Silver ink from Henkel was trialled on 10 prints of a 1m² printed circuit board (PCB) pattern. A polyester screen mesh was made with a mesh count of 180, as this was recommended on Loctite's 1010 ink data sheet. Printing was carried out by a flexible PCB manufacturer, who had the equipment at hand along with prior experience. There were two expected outcomes for this trial run: firstly, to prove the concept works on such large scale and secondly, to calculate the weight of ink required to print each 1m² product. The number of large flexible PCBs that are required annually is a known target to reach. This value is multiplied by the

grams of ink required for each product, in order to calculate the total amount of ink used annually. Annual ink requirements are passed onto the ink supplier, Loctite, to arrange bulk quotes.

Silver ink screen printing created excellent 1m² prototypes of serpentine flexible electrodes on base PET sheets. Images of these are confidential. This trial proved that silver ink is commercially ready to be used at this size and production scale. Having spoken to the ink suppliers mentioned above, a study or trial at this scale had never been attempted prior to this study.

Thermo-foldable ink trial

Thermo-formable ink will most likely not be commercially ready for another year; however, small samples of ink can be attained for testing. A technical representative at Henkel Ltd. Suggested that the standard Loctite 1010 Silver ink has some level of stretch, but had not been tested. To find out whether the stretch is enough for the required application, the ink was screen printed onto Acrylonitrile butadiene styrene (ABS). An ABS vacuum-forming supplier carried out the next process of forming the sheets into 3D moulded shapes. In order to minimise cost for this trial, the screen printing was carried out in house. The screen mesh was created by the squeegeeandink company, who provides a service that allows customers to email them a pattern of any size, which they return as professionally made screen. A special software is required to create the preformed 2D image which would conform to the 3D object perfectly as intended, after vacuum forming. But as this piece of software is very costly to own or use, it was not used for this trial.



Figure 15 Vacuum form ABS with screen printed silver ink

The silver ink performed better than expected, as it withstood the forming and heat well. However, more in the corners and anywhere that has been prone to high stress, resulted in crack as seen in Figure 15. This was a good test to try initially however the next step is to carry out the same process on Loctite's WIK20489-56A, which would resolve this issue as it has a higher polymer content and designed to withstand thermoforming. From this trial, it was concluded that Loctite 1010 can be used for thermo-folding, only when it is low level as too much stretch causes the ink to crack. When deep draw in the base material of the electrode is required, then Loctite has special Silver inks which allows for this extra stretch. However, the electrical conductivity and other properties may be decreased, which should be analysed when comparing specifications. From the results from this study, WIK20's lack of electrical conductivity made it difficult to investigate further in thermo-foldable inks. When ink manufacturers improve this, the study could revisit this experiment.

[PEDOT lithography](#)

Simple track-based patterns were developed on PEDOT:PSS films using photolithography for creating prototypes and testing. Calculating the theoretical electrical resistance is great to compare with practical values. Figure 16 on the left shows a serpentine pattern with track width and gap of 1.5 / 1 mm and on the right 1 / 1 mm, which is visibly harder to see. The left serpentine's total length is 508mm, therefore it consists of 338 electrical squares roughly. This PEDOT:PSS film has a sheet resistivity of 200 Ω , which works out to be 67k Ω for the total

serpentine. The measured practical resistance was $1.4\text{M } \Omega$, which is a 2388% increase. A full analysis of the lithography process is required to identify where the electrical resistance losses are occurring. $1.4\text{M } \Omega$ for such a small sample is far below the requirement, which is $4\text{k } \Omega$ for the full serpentine on a 1M square sheet.

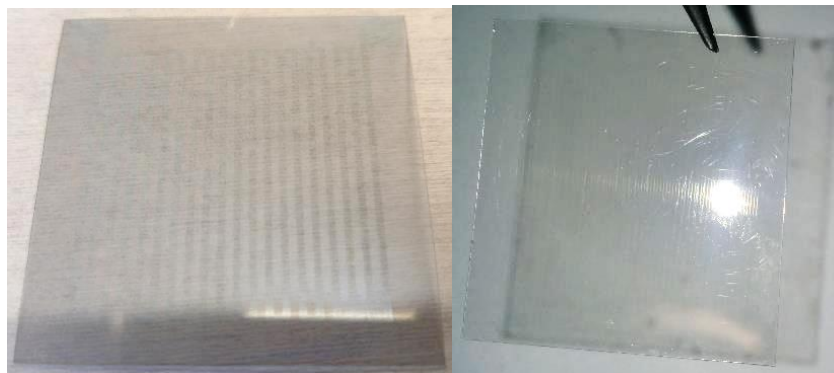


Figure 16 1 inch sample serpentine patterns created by photo-lithography

Photo-lithography

1. Photo resist (Cyclo-pentanone S1813 - Negative) is spin coated on top of the PP at a set thickness.
2. 30 seconds on the hotplate to semi-dry the resist.
3. A negative of the desired pattern is etched on the resist using a direct laser.
4. Dip in the developer (MF-319) which removes the laser exposed areas.
5. Completely etching the PEDOT:PSS can be carried out by either one of the following:
 - a. Dry process - Reactive Ion Etching (RIE)
 - b. Wet process – Dip in Sodium Hypochlorite
6. Finally, the left-over photo resist covering the required pattern is removed by submerging the substrate in Acetone. Acetone can fully dissolve any remaining S1813 whilst causing minimal damage to the PEDOT:PSS.

Reactive Ion Etching (RIE)

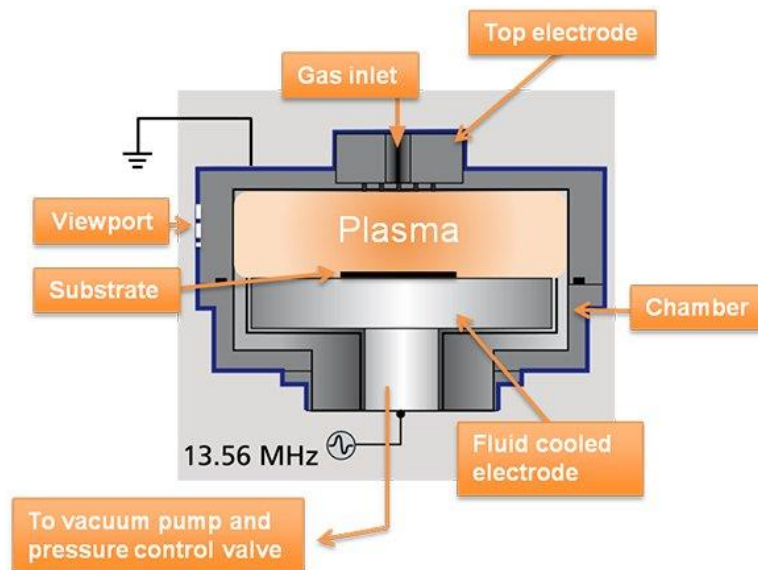


Figure 17 (Reactive Ion Etching (RIE) - Oxford Instruments)

Figure 17 shows a simple diagram of the RIE system. The three key elements of the system are: the chosen gas, radio frequency (RF) generator and vacuum chamber. As a general rule, the wafer platter, where you place your substrate, is situated in the bottom of the electrically-isolated chamber. The high RF electromagnetic field to the wafer platter, typically 12.56 Megahertz at a few hundred watts, ionises the gas in the chamber which in turn creates a plasma. The amounts and types of gas used is based on the etch required. Oxygen and Argon are the two main gases used when etching graphene, as they are proven to be completely removed after atomic force microscopy (AFM) inspection. (Mariana C. Prado, 2013)

PEDOT:PSS material testing and comparison with Graphene

Bend test

A general bend test was carried out on a sample of 5 tracks, each at a length of 5cm and a width of 1mm. The initial electrical resistance was measured using a multi-meter R0, before any bends. The measurement is repeated after each bend and the change in percentage is recorded. Figure 18 shows a how the percentage change in resistance, over 100 bends; for Copper, PEDOT:PSS and Graphene.

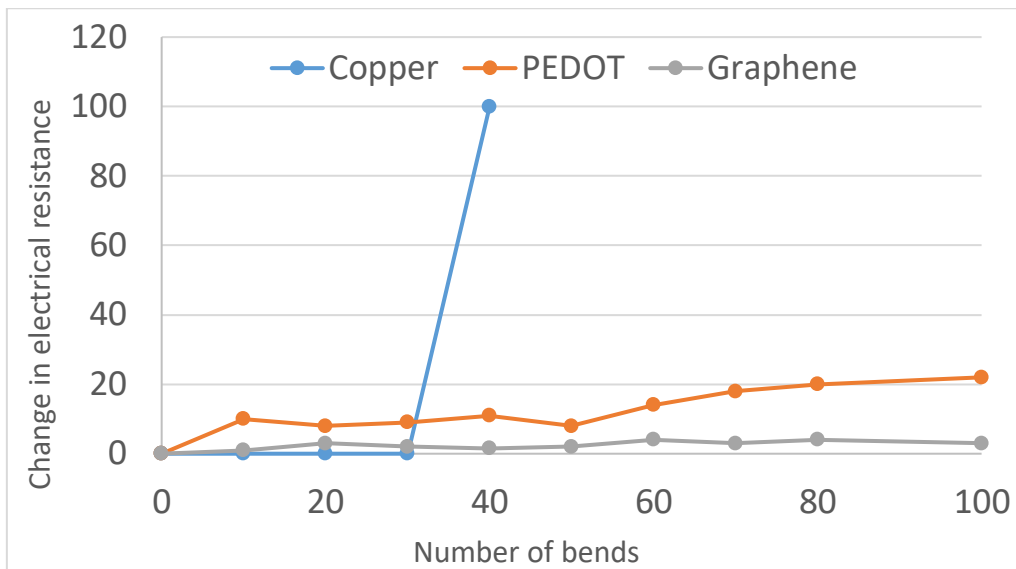


Figure 18 Electrical conductivity comparison

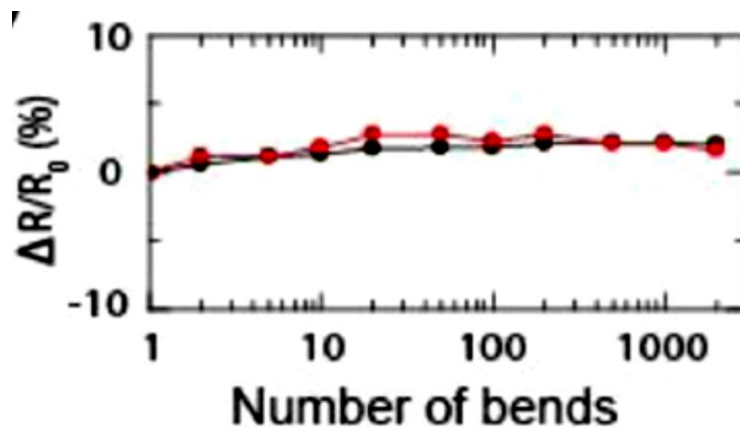


Figure 19 Graphene Bend Test (Bointon et al., 2015)

On the other hand, Graphene films measured a percentage difference lower than 4%, even after 1000 bends as shown in Figure 19. For this application robustness is a very important requirement, therefore Graphene would be the preferred material based on these results.

PEDOT:PSS Industrial large scale printing

Mayer Bar Coating

A uniform wire tightly winds a long rod, both made of stainless steel, as seen in Figure 20. The diameter of the wire can vary from 4.5um to 350um depending on the required coating thickness. The gaps between the coils determines the fine amount of coating that is applied to the substrate, as it moves along the rod. The thickness of the wet coat is 0.173 times diameter of the coil wire. Figure 21 show where the rod is placed in the system and how the reservoir of PEDOT:PSS ink

is applied on to the PET sheet, by passing through the rollers. This method is a relatively fast and uniform for applying inks such as PEDOT:PSS. Mayer Bar provides scalability at a low cost, without effecting the quality. These are some the methods that new materials such as Graphene must compete with, to be able to break into the real market.

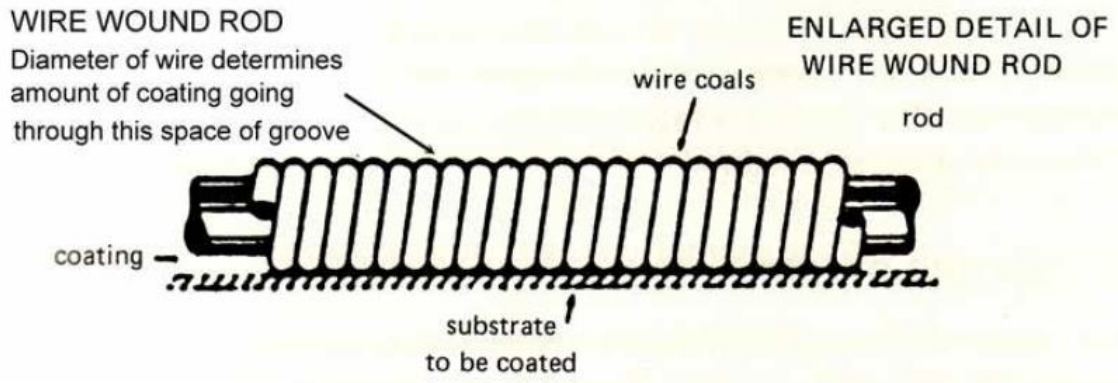


Figure 20 Mayer bar stainless steel rod

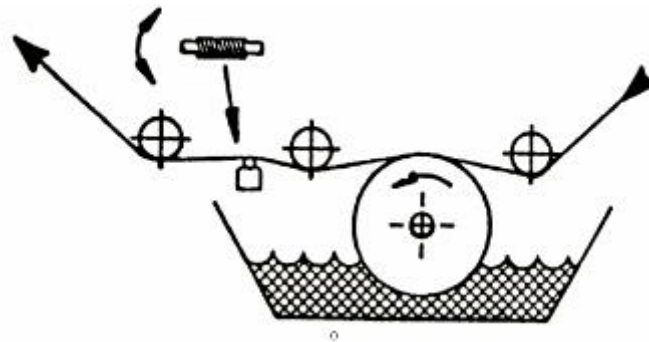


Figure 21 Mayer bar coating

Subtractive printing

Kimoto Tech Georgia USA provided pre-coated PEDOT:PSS PET films. The PET is plasma treated to aid the adhesion, prior to the PEDOT:PSS coating on a 1.27m width roll, using Mayer bar technology and other proprietary techniques. The width of the roll may be cut to any width that is required. However, this runs the risk of creating waste; which would cost the customer.

A4 samples of PEDOT:PSS PET, from Kimoto Tech; came as sheets of $200 \Omega/\square$ and $600 \Omega/\square$. The patterning on these sheets was carried out at Yeovil Circuits using their current screen printing setup:

1. UV photoresist is screen printed onto the PEDOT:PSS sheet. The screen consists of the required pattern.

2. The resist is cured on a conveyer belt under UV radiation, for a fixed time of 7 seconds. This is based on the energy needed for the resist to be fully cured, stated on the data sheet.
3. The etching is carried out in a bath of Sodium Hypochlorite for 10 seconds, which is enough to remove the exposed or uncovered PEDOT:PSS. However, 5 seconds for a 1% concentrate of Sodium Hypochlorite will deactivate the conductivity as explained on the 'PEDOT:PSS' paragraph.
4. The sheets should be rinsed with water to remove the Sodium Hypochlorite and halt the etching.
5. Next, the resist covering the required PEDOT:PSS pattern must be removed, which is done by using a bath of resist stripper.
6. A final water rinse removes the stripper, leaving behind the desired pattern of PEDOT:PSS.

Photos of A4 PEDOT:PSS patterns have not been added here as the patterns are confidential. Carrying out this experiment was time consuming as it was important to clean away all the etchant before stripping the resist. These steps are common in the lab, but applying it to large samples come with a whole new set of difficulties. Only 2 out of 10 samples were etched correctly, so as the success rate of this method was low, other methods are investigated.

Additive printing

Heraeus Holdings does a range of screen-printable PEDOT:PSS paste under the name of Clevios. PEDOT:PSS does not naturally adhere well to surfaces, therefore it would have taken some time to develop the Celvios paste.

Clevios S V3 STAB and S V4 STAB screenprints on glass

paste	S V3 STAB	S V3 STAB	S V3 STAB	S V3 STAB	S V4 STAB	S V4 STAB	S V4 STAB	S V4 STAB
mesh/dia.	500/24	355/31	355/31	355/31	500/24	355/31	355/31	355/31
passes	1	1	2	3	1	1	2	3
SR (ohm/sq)	652	462	264	146	504	328	166	108
transm. (%)	86,8	85,9	80,2	75,0	87,0	86,0	80,3	75,1
haze (%)	1,1	1,3	1,7	1,9	0,9	1,2	1,4	1,6
thickn. (nm)	192	256	492	836	202	315	595	838
R _a (nm)	7	9	7	15	12	12	13	14

Figure 22 (Heraeus, 2013)

Figure 22 shows the specifications of 2 different Clevios versions, S V3 STAB and S V4 STAB, applied using various screen mesh types at 1, 2 or 3 layers of coating. Applying any more than 1 coat increases the production complexities

due to coating, drying, and re-aligning. So, the ideal electrical resistance vs transmittance would be 1 layer of S V4 STAB.

In an industrial setup, the standard screen printing technique is used. This was carried out at a Yeovil Circuits Ltd as they have full scale facilities to screen print 1m². Their semi-automatic screen printing tool provided excellent uniform coatings. Samples were air dried, oven dried and UV cured. Oven drying achieved the best electrical conductivity, as the heat would have completely removed the insulating solvents from the paste.

Inkjet/Spray Printing

Cost of Conductive Ink

DuPont, SunChemicals and Henkel were the three different suppliers that were chosen to compare specification and cost of their various conductive inks. It was an easy win for Henkel Loctite EC1 1010 silver ink formulation, as it showed the lowest electrical resistance of 0.007 Ω/\square at like for like coating thickness, and the lowest in cost at £0.018 / gram. SunChemical's CHSN8013 costs £0.644 / gram, with a sheet resistance of 0.011 Ω/\square . And DuPont's PE827 cost £0.79 / gram with a resistance of 0.06 Ω/\square .

Drying & Curing

Another important specification is the drying method and time. This is important for the printing supplier, as UV drying or curing needs far less time compared to IR blow drying and oven drying. Current Silver based inks seem to only dry using IR blow drying, which would need Yeovil Circuits Ltd to buy an IR conveyor belt blow drying equipment and allow extra time for this process compared to their current process. However, recently in March 2017, SunChemical published a data sheet of a new UV based flexographic Silver ink C2110414D7. (SunChemical, 2017) This ink has a higher sheet resistivity of 4 to 22 Ω/\square depending on the treatment applied on the base PET film. However, as it uses UV curing, the drying time is much lower, which can be a huge benefit in the overall process. As the ink is designed for flexographic printing, the viscosity is set to a low 1.2 - 2.2 Pa s, compared to 9 Pa s for Henkel's Loctite 1010 screen printable Silver ink. This ink has a higher sheet resistivity of 4 to 22 Ω/\square depending on the treatment applied on the base PET film. However, as it uses UV curing, the drying time is much lower, which can be a huge benefit in the overall process. As the ink is designed for flexographic printing, the viscosity is set to a low 1.2 -

2.2 Pa s, compared to 9 Pa s for Henkel's Loctite 1010 screen printable Silver ink.

LDS experimental

In an attempt to recreate and improve the LDS technology as described in the introduction, an experiment to disperse GO in a polymer matrix was carried out. A study on GO-polymer nanocomposites was found, which follows the procedure shown below on Figure 23. (Liu and Zhang, 2015)

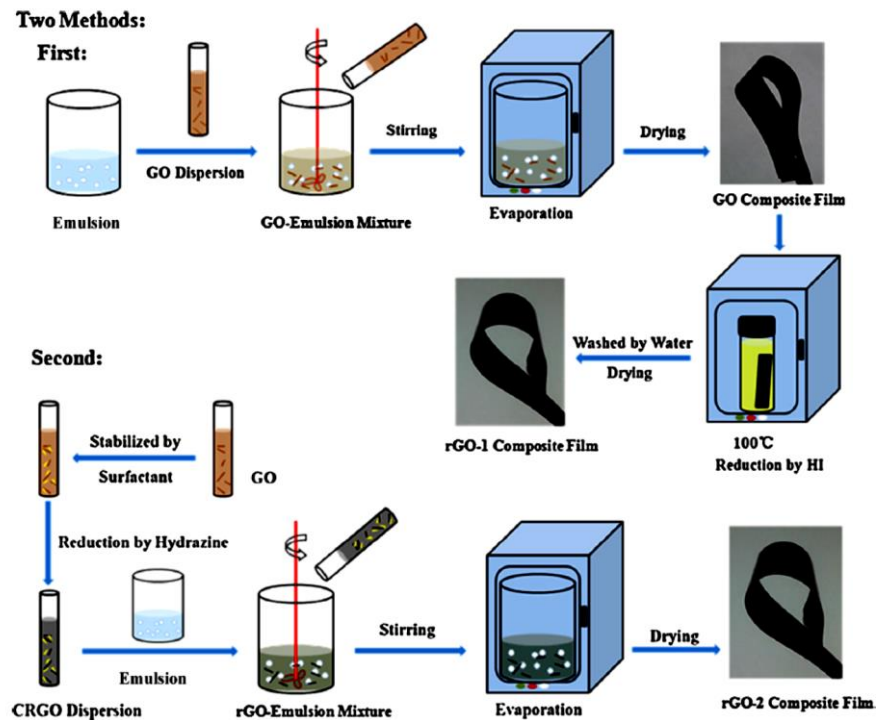
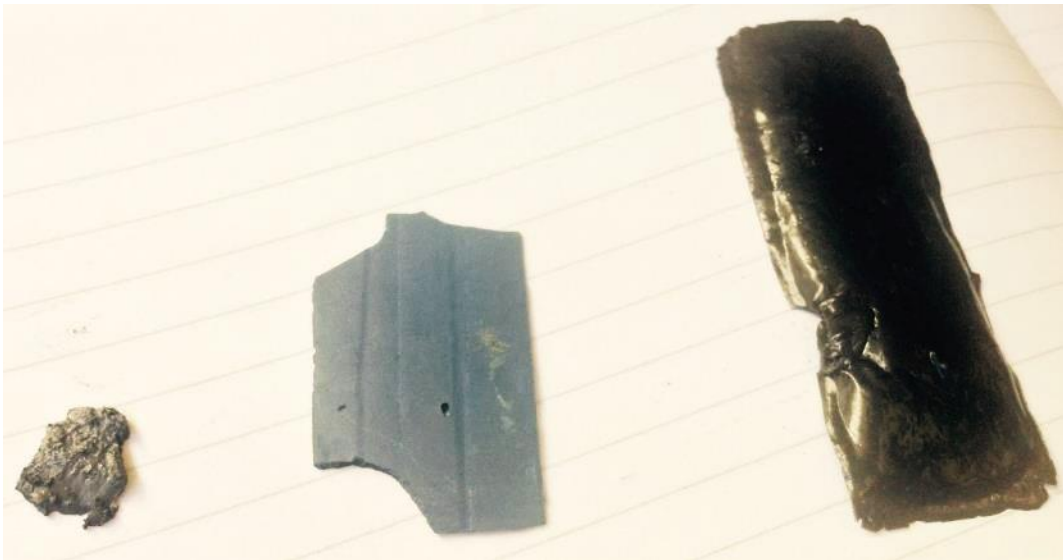


Figure 23 GO-Polymer Nanocomposite

A similar setup was carried out for this research, where GO from Graphenea was mixed with Acrylic Styrene (AS) from SunChemicals, which created a solid yet flexible membrane once dried. The ratio between GO and AS decides the flexibility of the membrane.



The membranes were passed under a 60mW green laser light for several hours, however there was no sign of rGO after analysing the sample under Raman spectroscopy. The low consistency on GO, and a larger ratio of AS, may have been the reason for this negative result. It was clear that a much larger amount of GO would be needed to create electrically conductive tracks. However, this limits the flex in the membrane. LPKF is a company that specialises in LDS technology. LPKF coats a thin layer of metal-oxide onto a solid moulded substrate, then later reduces the oxide to create tracks. The laser that LPKF uses is far more powerful and precise, with the aid of a computer. Even if a fine-tuned GO-AS mixture was created in this study, there would still be a lack of laser power which LPKF sells along with its IP, as a subscription basis.

LPKF sells the computer aided laser device, tubs of metal-oxide paste and rights to use their technology, in one package.

Electronics

Time-domain Reflectometry (TDR)

When an electronic wave is sent through an impedance matched wire with an open circuit end, a reflection wave is sent back to the source. Figure 24 shows a simple diagram of this setup, with an oscilloscope to view both the transmitted and reflected wave. Note that the signal source and transmission line has a matched impedance of 50Ω . However, the oscilloscope is attached with a much higher impedance of $1M\Omega$ to ensure that it does not affect the main transmission line. Any small discrepancy in the line would cause unwanted reflections. Therefore, it is key that the only discrepancy occurs at the end of the line, hence the open circuit (infinite impedance).

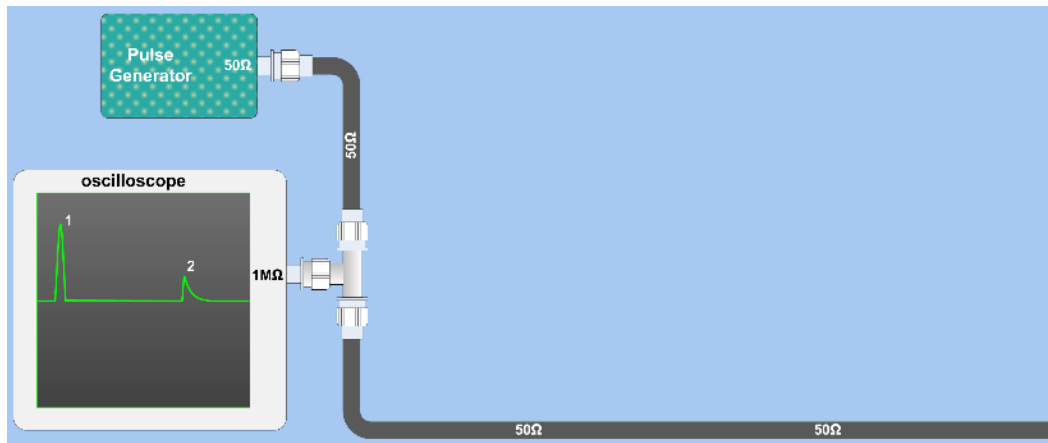


Figure 24 A simple TDR workbench setup

The time between the incident and reflected wave is the measure of time taken for the wave to travel from the source to the open circuit and back.

Equation 1 is used to calculate the length of wire which is the useful information needed for this project.

Equation 1

$$TDR\ Length = \frac{c * v * T_d}{2}$$

C = Speed of light 10^8 m/s

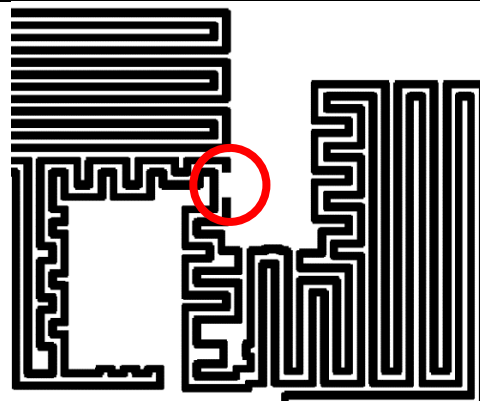
V = Velocity factor of transmission line

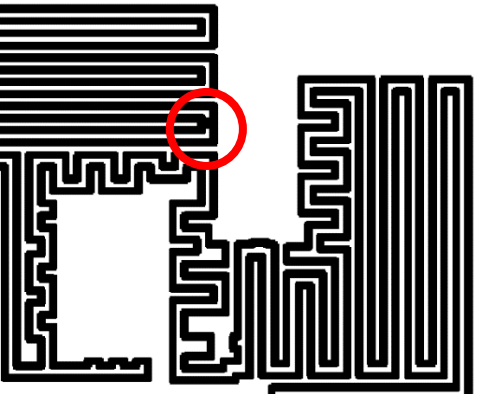
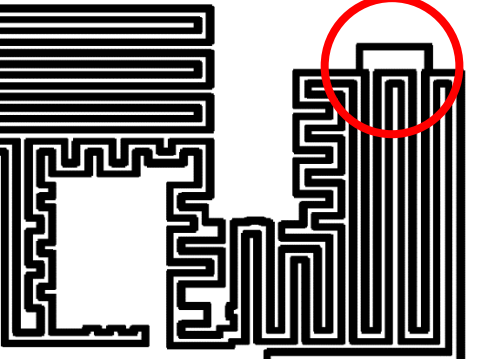
T_d = Round trip time between sent pulse and first reflection

TDR can be used to sense three distinct types of tamper that could occur in a security safe or environment. They are described in detail below.

A break in the line

The incident wave would be reflected much earlier than expected, as the track length is shortened.



<p>Short circuit between other lines</p> <p>If there are multiple tracks each on a separate TDR network, a short between them would cause signal to cross.</p>	
<p>Extended or shorter bypass line</p> <p>When a large section of the track is bypassed, some of the signal would arrive sooner.</p>	

When a 'step' signal generator is used in a TDR system, the reflections can take various forms depending on how the end of the wire is terminated. Figure 25 highlights the different reflection types, which varies depending on whether there is an open circuit, short circuit, inductive distortion, capacitive distortion, or matched impedance. Touching the track, or even passing a human hand across over, creates many distortions that can be monitored on an oscilloscope.

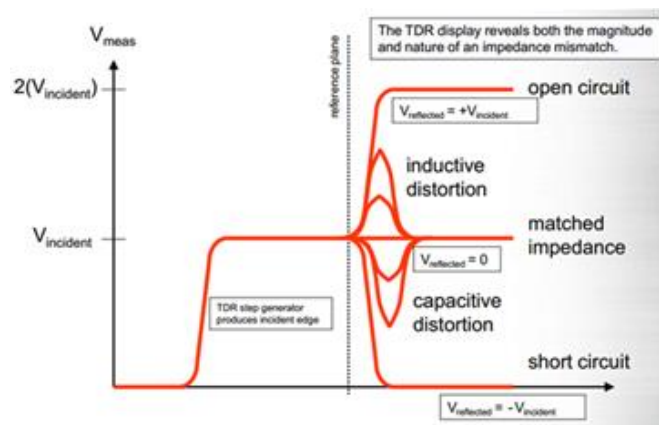


Figure 25 Various TDR reflection waves, $V = \text{Voltage}$. (Emworks, 2017)

Other signal wave forms such as sine, produces an alternative set of reflections.

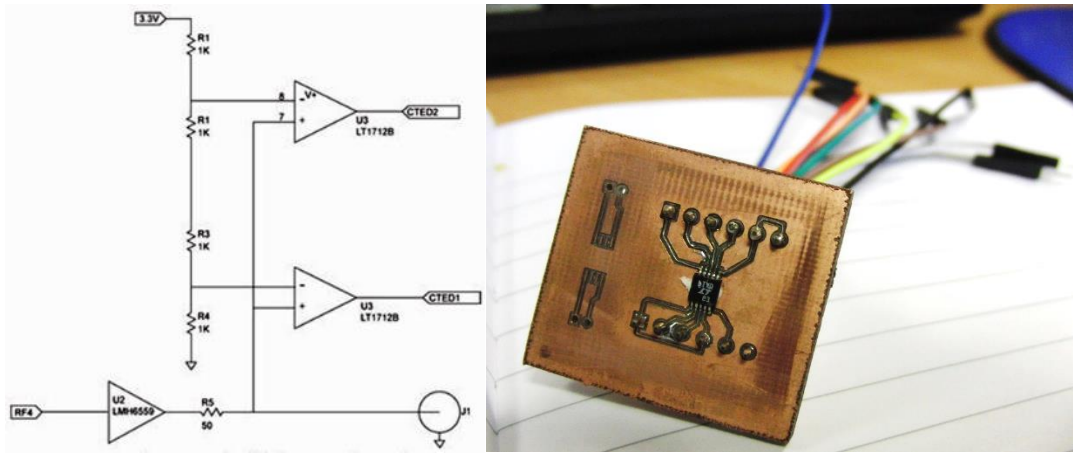


Figure 26 Trigger circuitry

This setup uses an open circuit end, where the reflection is added as voltage on top of the incident wave, thus creating a step as described previously. A PCB was designed, milled out - Figure 26 right, and then coupled with a microcontroller to create a TDR length monitoring system. The first part of the system monitors the incident and reflection waves, which trigger two other waveforms Figure 26 left: one is triggered by the incident wave and the other by the reflected wave. These are determined by a potential divider that only powers up an operational amplifier, if the correct voltage is reached.

Figure 27 on the left shows where the two trigger points occur on the step wave (Jim Bartling, 2009) [OBJ] and on the right, all three signals occur on the device that was made for this study.

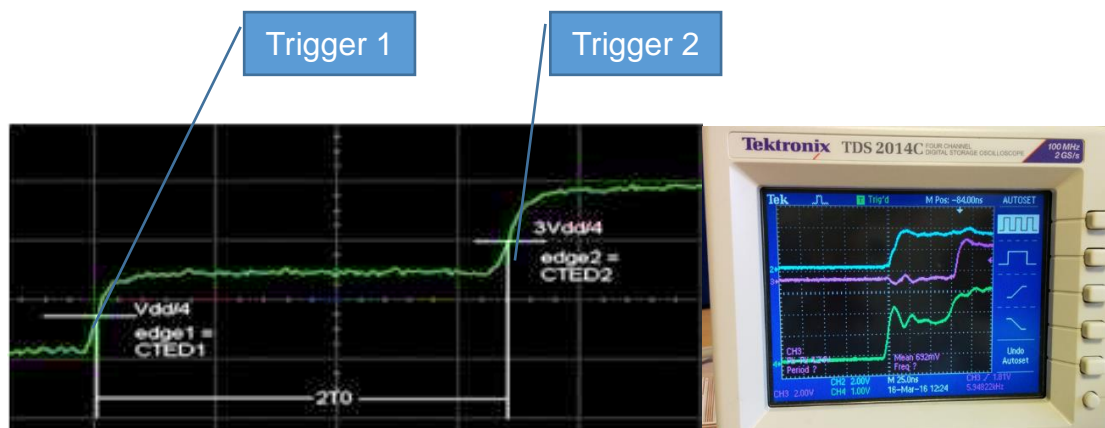


Figure 27 All the signals from a TDR system on the right.

The second part of the TDR system consists of a microcontroller from Microchip Technology. The feature that was required to complete the TDR is the Charge

Time Measurement Unit (CTMU) is on the AN1375 chip. A CTMU evaluation board was purchased, as it contains the CTMU functions, along with a few user interfaces such as LEDs, ADC, and programming controllers. Evaluation boards are generally used to create quick prototypes for proof of concept. However, a bespoke PCB would be made with the actual devices or features in use, which dramatically lowers size and cost.

The two waves from the op-amps are fed into a controlled NOR gate which waits for the incident wave to occur before accepting the reflection wave. Upon receiving a pulse signal from the incident wave, a switch (SW) is turned on, then later closed by the reflection pulse. The switch commence flow from a constant current source to a capacitor in the Analog to digital converter (ADC). Effectively, the capacitor is charged for the exact time it takes for the incident wave to transmit and reflect (see Figure 28).

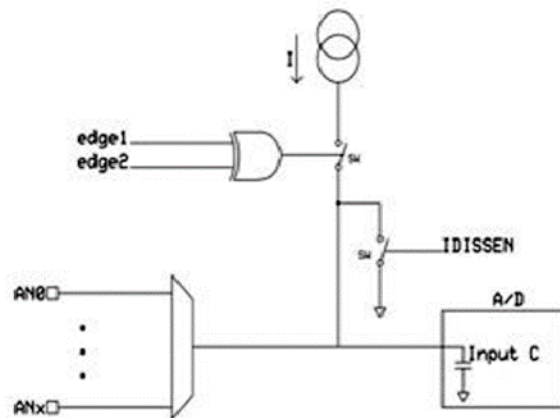


Figure 28 Internal circuitry of the microcontroller

Equation 2

$$t = \frac{VC}{I}$$

t = Time (Calculated in code)	C = Capacitance (Fixed)
V = Voltage (Calculated internally)	I = Current (Set)

As the ADC can only read voltage across the internal capacitor, time (t) would have to be calculated using Equation 2. Here, you can see why it is important to use a constant current source.

Time (t) can now be using in place of T_d to calculate the TDR length using Equation 1.

Algorithm

Flag 1 – Detected incident wave

Flag 2 – Detected reflection wave

1. Set up UART (Output to terminal)
2. Set up CTMU (Set up to automatically open switch when flag 1 is set and close switch when flag 2 is set)
3. Set up ADC
4. Main
 1. Clear flag 1 & flag 2
 2. Set PIN A High (Signal-out)
 3. Wait for Flag2
 4. Sample Capacitor's (Voltage) in the ADC
 5. End sampling, convert, store in register
 6. Output register to UART (Terminal)
 7. LOOP

See appendix for the full code.

TDR Summary

A step pulse is sent down a serpentine copper track, which is not terminated (open circuit). This causes a reflection at the end of the track, which is sent back and seen overlapping the source pulse. The TDR electronics differentiate between the two and subsequently, the time delay is measured using a microcontroller running software. The software inputs all known values into

Equation 1, then displays the calculation onto a screen. With this value, tamper on the tracks can be identified with greater information compared to a standard tamper circuit.

Patterns

An investigation into various patterns for tamper security was carried out. The most common pattern is in the shape of serpentine track across the device, as seen on Figure 29 (David D. Eaton, David R. Staab, Ruben C. Zeta, 2011)

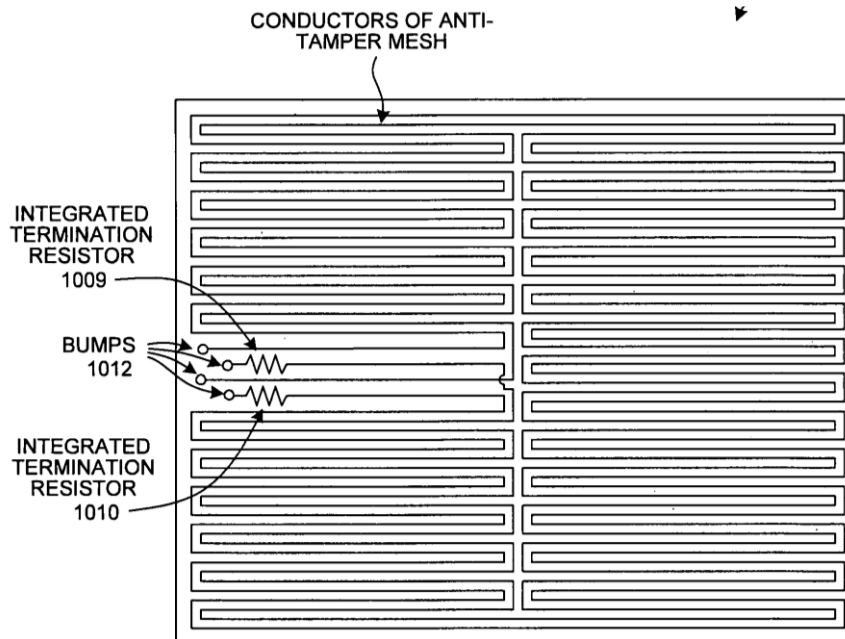


Figure 29 (David D. Eaton, David R. Staab, Ruben C. Zeta, 2011)

It was thought that there could be many other patterns that may increase the coverage, as well as the difficulty in breaking through. One simple method of increasing tamper resistance is by making the serpentine track and gap narrower. This increases the coverage and makes it harder for an attacker to follow around the track.

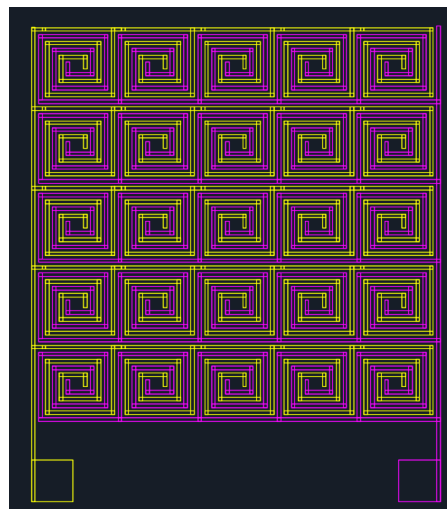


Figure 30 Capacitive spiral pattern, each colour is an isolated terminal

Figure 30 was inspired by (Hooper et al., 2014) ^[OBJ] a study on an extreme form of sub-wavelength wave guide, which uses a chain of conducting spirals to support wavelengths many times longer than any other geometry. The pink track and the yellow track do not cross at all, and therefore creates a 2-dimensional capacitor. In an attack, a short between the track could easily occur or there could be a

break within a track. This would alter the capacitance between the two and this can be monitored in real time using electronics.

This pattern was screen printed and tested, for the hope to measure a significant capacitive change, when one spiral in the pattern is physical tampered with. Unfortunately, each spiral only made up a small percentage of the total capacitance. Therefore, cheap low-resolution microcontrollers would not be able to monitor this difference. Even if a device with a higher resolution is used, small changes get masked by the parasitic or stray capacitance in the system; which is mainly caused by external objects such as movement of the PET substrate. As the full size of the product is required to be a rough size of 1 metre square, large fluctuation would be even higher, consequently hiding any tamper.

Ladder Network

As the length of each track is the main factor that deters the total electrical resistance, an idea of creating a ladder pattern, as seen in Figure 31.

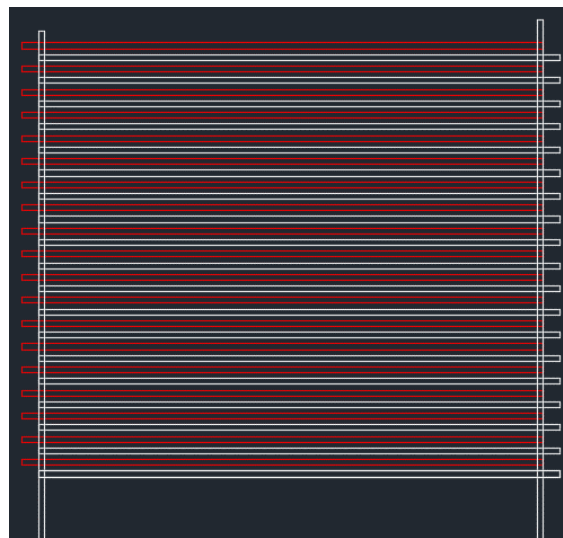


Figure 31 Ladder pattern, designed on AutoCAD

This pattern would use a resistance measurement electronics system, which measures electrical resistance at a given frequency between each side. A broken track would increase the resistance, thereafter alarming the main PCB. It was identified that, the larger the ladder network, the smaller the monitored change in resistance. As the total size required for the product is large, this ladder network would not show a meaningful change in electrical resistance; upon tamper. Therefore, this pattern was no longer investigated. That said, it is possible to use high precision resistance measurement systems, but this gets larger in size with increases in cost, make it unviable for this project.

Conclusion

The main aim of this project is to scale up graphene so it could be used as an electrode on a substrate size of one metre squared. Spinnaker needs about 3000 of these sheets per annum, and as liquid exfoliation is currently the closest match for high scalability over other methods, this was the process that was investigated the most. It was concluded that liquid exfoliation on graphite creates few layer graphene (FLG) solutions, and FLG is more comparable to graphite than Graphene with its desired properties. A small percentage of mono and bi layers are present in the final solution; however, it is not a significant amount to increase electrical conductivity. Due to this reason, research on Graphene was put on hold until a scalable solution merges in the future. Many large corporations are working on large scale, roll-to-roll chemical vapour deposition (CVD) graphene. Regrettably, time and funding were the two limitations on this project, to overcome the current barriers of scaling up graphene.

Graphene has a long way to go until its wonderful features can be fully exploited in the industry. When scalability and quality of graphene is consistent, all the various applications that have been researched worldwide, would come into significant use. For the time being, other materials such as Silver ink show a promising sign in the flexible PCB industry. Mainly due to its relatively low cost and its workable electronic values, which are currently the main drivers for any company who creates portable battery powered products. If battery cell technology was improved, then the interesting abilities of new materials with high electrical resistance could be tapped. Having created a full size 1m² silver ink printed PCB prototype, to use with a newly developed electronic sensing system; is a great outcome for this study. Silver ink is not relatively cheap and very easy to screen printing, providing the right equipment is also attained. Curing Silver ink, the step that removes the solvents; which increases the conductivity, could still be improved. Legacy processes, prefer UV curing as the time taken is seconds over minutes under IR radiation. However, by using Silver ink, many other lengthy steps have been eliminated; such as etching and stripping resist. Silver ink can be printed as thin as 10um whilst retaining an electrical resistance of 10uΩ. Being so thin added an extra security feature, compared to copper sheet electrodes. PEDOT:PSS has an advantage when it comes to its transparency, however its conductivity must be improved greatly for use in battery powered portable products. The newly developed electronics sensing system proved to be

a great advanced as you can not only sense a simple break in the electrode, but any smart tamper that involves rewiring. The system also provides information on the area where the tamper has occurred. And if the sensitivity is increased by a simple code change in the software, other benefit can also be achieved. This technology is also the foundation of future tech such as machine learning. Software could be installed where artificial intelligence (AI) would identify normal use to an attack. The work on various pattern shapes proved that the best pattern for a security tamper circuit is a serpentine, as using any other patterns does not give the same level of coverage. It would be wise to revisit Graphene and other 2D materials such as Transition metal di-chalcogenide monolayers (TMDC's), in the next few years.

References

- AGFA (2001) *Patterning Orgacon™ film by means of UV lithography: Application sheet* (accessed 14 March 2017).
- Alemu D, Wei H-Y, Ho K-C and Chu C-W (2012) Highly conductive PEDOT: PSS electrode by simple film treatment with methanol for ITO-free polymer solar cells. *Energy & Environmental Science* 5(11): 9662.
- Bointon TH, Barnes MD, Russo S and Craciun MF (2015) High Quality Monolayer Graphene Synthesized by Resistive Heating Cold Wall Chemical Vapor Deposition. *Advanced Materials* 27(28): 4200–4206.
- David D. Eaton, David R. Staab, Ruben C. Zeta (2011) *Patent US7868441 - Package on-package secure module having BGA mesh cap*. Available at: <https://www.google.com/patents/US7868441> (accessed 17 May 2017).
- Davim JP (2012) *Tribology in manufacturing technology*. Berlin, New York: Springer.
- Emworks (2017) *TDR of connectors*. Available at: <https://www.emworks.com/application/tdr-of-connectors> (accessed 6 September 2017).
- Graphenea (2017) *Properties of Graphene*. Available at: <https://www.graphenea.com/pages/graphene-properties#.WZHv-3G1vDc> (accessed 14 August 2017).

- Gwent Group (2017) *The Gwent Group, Leaders in paste manufacturing, sensor/biosensor development and Instrumentation* Available at: http://www.gwent.org/gem_screen_printing.html#screen (accessed 4 September 2017).
- Henkel (2016) Loctite ECI 1010.
- Heraeus (2013) Clevios S V3 & V4 STAB layer thickness 13-04-02 (accessed 18 May 2017).
- Hooper IR, Tremain B, Dockrey JA and Hibbins AP (2014) Massively sub-wavelength guiding of electromagnetic waves. *Scientific reports* 4: 7495.
- James C. Y. Watt, Anne E. Wardwell, Morris Rossabi (1999) *Why Ancient Silk Is Still Gold: Issues in Chinese Textile History on JSTOR*. Available at: https://www.jstor.org/stable/4629553?seq=1#page_scan_tab_contents (accessed 4 September 2017).
- Jim Bartling (2009) *Low-Cost, High-Resolution Time-Measurement Application*.
- Koenig SP, Boddeti NG, Dunn ML and Bunch JS (2011) Ultrastrong adhesion of graphene membranes. *Nature nanotechnology* 6(9): 543–546 (accessed 11 January 2017).
- Liu L and Zhang D (2015) The sensitive electrical response of reduced graphene oxide–polymer nanocomposites to large deformation. *Composites Part A: Applied Science and Manufacturing* 75: 46–53.
- Mariana C. Prado (2013) Optimization of graphene dry etching conditions via combined microscopic and spectroscopic analysis (accessed 5 September 2017).
- S. Mitura, K. Mitura, P. Niedzielski, P. Louda, V. Danilenko (2006) Nanocrystalline diamond, its synthesis, properties and applications (accessed 14 December 2017)
- Neves AIS, Bointon TH, Melo LV, Russo S, Schrijver I de, Craciun MF, et al. (2015) Transparent conductive graphene textile fibers. *Scientific reports* 5: 9866 (accessed 15 February 2017).
- Ramalingam P, Pusuluri ST, Periasamy S, Veerabahu R and Kulandaivel J (2013) Role of deoxy group on the high concentration of graphene in surfactant/water media. *RSC Advances* 3(7): 2369.
- Reactive Ion Etching (RIE) - Oxford Instruments*. Available at: <https://www.oxford-instruments.com/products/etching-deposition-and-growth/plasma-etch-deposition/rie> (accessed 11 May 2017).

SunChemical (2017) *UV Silver C2110414D7*. Available at: http://www.gwent.org/gem_data_sheets/polymer_systems_products/flexographic_inks/uv_silver_c2110414d7.pdf (accessed 12 June 2017).

Bibliography

Blankschtein, D., Chih-Jen, S., Micheal, S. S. & Shangchao, L., 2010. Understanding the Stabilization of Liquid-Phase-Exfoliated Graphene in Polar Solvents: Molecular Dynamics Simulations and Kinetic Theory of Colloid Aggregation. *JACS ARTICLES*.

Chung-An, W. et al., 2011. Dispersion of graphene in aqueous solutions with different types of surfactants and the production of graphene films by spray or drop coating. *Journal of the Taiwan Institute of Chemical Engineers*, pp. 140-146.

Dietz, K., 2012. *Karl's Tech Talk: Copper Surface Preparation for Dry Film Lamination, Part A*. [Online] Available at: <http://flex.iconnect007.media/index.php/article/67534/karls-tech-talk-copper-surface-preparation-for-dry-film-lamination-part-a/67537/?skin=flex> [Accessed 1 July 2015].

Ferrari, A., 2006. Raman Spectrum of Graphene and Graphene Layers. *PHYSICAL REVIEW LETTERS*.

GHAFFARZADEH, D. K., 2012. *IDTechEx Forecasts a \$100 Million Graphene Market in 2018*. [Online] Available at: http://www.electronicproducts.com/Analog_Mixed_Signal_ICs/Amplifiers/IDTechEx_Forecasts_a_100_Million_Graphene_Market_in_2018.aspx [Accessed 16 July 2015].

Hummers, W. S. & Offeman, R. E., 1958. Preparation of graphite oxide. *Baroid Division*, p. 1339.

Innovia Security Pty Ltd, 2014. *Guardian® - Facts and Figures*. [Online] Available at: <https://www.innoviasecurity.com/guardian-facts-and-figures/> [Accessed 30 June 2015].

Koenig, S. P., Boddeti, N. G., Dunn, M. L. & Bunch, J. S., 2011. Ultrastrong adhesion of graphene membranes. *Nature*, Volume 6, pp. 543-546.

Lucia, B. & Robin, J. C., 2001. Library of FT-Raman spectra of pigments, minerals, pigment media and varnishes, and supplement to existing library of

Raman spectra of pigments with visible excitation. *Spectrochimica Acta Part A*, Volume 57, p. 1491–1521.

Mrmak, N., 2014. *Graphene properties*. [Online] Available at: <http://www.graphene-battery.net/graphene-properties.htm> [Accessed 30 June 2015].

NiTEC, 2015. *Electroless Nickel Plating, corrosion resistance and surface technology specialists*. [Online] Available at: <http://www.electroless-nickel-plating.co.uk/technical-information-corrosion-resistance-nickel-plating-company.php> [Accessed 01 July 2015].

Paton, K. R., 2014. Scalable production of large quantities of defect-free few-layer graphene by shear exfoliation in liquids. *Nature materials*, 13(1), pp. 624 - 630.

Pu, N. W. et al., 2012. Dispersion of graphene in aqueous solutions with different types of surfactants and the production of graphene films by spray or drop coating. *Journal of the Taiwan Institute of Chemical Engineers*, Issue 43, pp. 140-146.

Senese, F., 2010. *What is electroless plating?*. [Online] Available at: <http://antoine.frostburg.edu/chem/senese/101/redox/faq/electroless-plating.shtml> [Accessed 2015 July 01].

The university of wisconsin, 2010. *Stereolithographed Microwave Components*. [Online] Available at: <http://cmb.physics.wisc.edu/stereolithograph/index.html> [Accessed 01 July 2015].